CHEMISTRY OF MATERIALS

VOLUME 18, NUMBER 19 SEPTEMBER 19, 2006

Communications

Electrochemical Synthesis of Yttrium Oxide Nanotubes

Vishnu V. Rajasekharan and Daniel A. Buttry*

Department of Chemistry (3838), University of Wyoming, 1000 East University Avenue, Laramie, Wyoming 82070

Received May 3, 2006
Revised Manuscript Received August 7, 2006

Inorganic nanomaterials are attracting a great deal of attention due to their many potential applications in the fabrication of electronic devices, sensors, biochips and energy-storage media.[1−12] They often have unusual characteristics that can be amplified by their nanoscale size and sometimes exhibit marked shape-specific effects.[12] Generally, oxide nanotubes are synthesized either by template[13] or by hydrothermal processes.[14] Because these synthetic procedures place significant restrictions on the growth conditions, it is desirable to examine new routes to such materials.[12] Electrochemical methods have been shown to be suitable for synthesis of novel nanostructured materials under mild reaction conditions.[5,6] This communication will focus on synthesis of yttrium oxide (Y_2O_3) nanotubes using a novel nonaqueous electrochemical method that involves oxide transfer to Y(III) precursors.

Yttrium has both atomic and ionic radii lying close to the corresponding values of common rare earth emitter ions, like terbium, dysprosium,[15] and europium,[16] used in the phosphor industry. Thus, Y_2O_3 is a widely used host matrix for these emitters. A key requirement in this regard is that the films contain no OH^-, because it quenches emission from some rare earth ions.[17] Because of this, the synthetic conditions described below for depositing Y_2O_3 were designed to avoid the production of OH^- by directly producing oxide phases. This is achieved by electrochemical reduction of oxygen atom transfer reagents under nonaqueous, aprotic conditions in the presence of Y(III) precursors.

Oxygen atom transfer to a metal center is a common reaction in inorganic chemistry.[18] Generally, the metal oxidation state increases by two units for each O-atom transfer.[18] In contrast, the approach described here for cathodic electrodeposition of yttrium oxide employs elec-

(1) Gal-Or, L.; Silberman, I.; Chaim, R. *J. Electrochem. Soc.* **1991**, *138*, 1939−1942.
(2) Hu, Z.; Oskam, G.; Penn, R. L.; Pesika, N.; Searson, P. C. *J. Phys. Chem. B* **2003**, *107*, 3124−3130.
(3) Levy, P.; Leyva, A. G.; Troiani, H. E.; Sanchez, R. D. *Appl. Phys. Lett.* **2003**, *83*, 5247−5249.
(4) Natter, H.; Hempelmann, R. *J. Phys. Chem.* **1996**, *100*, 19525−19532.
(5) Penner, R. M. *J. Phys. Chem. B* **2002**, *106*, 3339−3353.
(6) Phillips, R. J.; Golden, T. D.; Shumsky, M. G.; Switzer, J. A. *J. Electrochem. Soc.* **1994**, *141*, 2391−2402.
(7) Sekita, M.; Iwanaga, K.; Hamasuna, T.; Mohri, S.; Uota, M.; Yada, M.; Kijima, T. *Phys. Status Solidi B* **2004**, *241*, R71−R74.
(8) Silver, J.; Martinez-Rubio, M. I.; Ireland, T. G.; Fern, G. R.; Withnall, R. *J. Phys. Chem. B* **2001**, *105*, 948−953.
(9) Tissue, B. M. *Chem. Mater.* **1998**, *10*, 2837−2845.
(10) Xiao, Z.-L.; Han, C. Y.; Kwok, W.-K.; Wang, H.-H.; Welp, U.; Wang, J.; Crabtree, G. W. *J. Am. Chem. Soc.* **2004**, *126*, 2316−2317.
(11) Xu, A.-W.; Fang, Y.-P.; You, L.-P.; Liu, H.-Q. *J. Am. Chem. Soc.* **2003**, *125*, 1494−1495.
(12) Yada, M.; Taniguchi, C.; Torikai, T.; Watari, T.; Furuta, S.; Katsuki, H. *Adv. Mater. (Weinheim, Ger.)* **2004**, *16*, 1448−1453.
(13) Lakshmi, B. B.; Dorhout, P. K.; Martin, C. R. *Chem. Mater.* **1997**, *9*, 857−862.
(14) Fang, Y.-P.; Xu, A.-W.; You, L.-P.; Song, R.-Q.; Yu, J. C.; Zhang, H.-X.; Li, Q.; Liu, H.-Q. *Adv. Funct. Mater.* **2003**, *13*, 955−960.
(15) Cotton, F. A.; Wilkinson, G. *Advanced Inorganic Chemistry*, 4th ed.; John Wiley & Sons: New York, 1980.
(16) McKittrick, J.; Bacalski, C. F.; Hirata, G. A.; Hubbard, K. M.; Pattillo, S. G.; Salazar, K. V.; Trkula, M. *J. Am. Ceram. Soc.* **2000**, *83*, 1241−1246.
(17) Soga, K.; Wang, W.; Riman, R. E.; Brown, J. B.; Mikeska, K. R. *J. Appl. Phys.* **2003**, *93*, 2946−2951.
(18) Holm, R. H. *Chem. Rev. (Washington, DC, U.S.)* **1987**, *87*, 1401−1449.

10.1021/cm061024t CCC: $33.50
Published on Web 08/26/2006

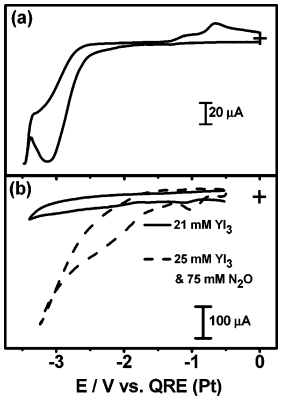

Figure 1. (a) CV of 46 mM N_2O. Scan rate, 200 mV/s; working electrode, Au (0.515 mm^2); solvent, DMF (0.1 M TBAP). (b) CV of N_2O in the presence of YI_3 (dotted line). Scan rate, 200 mV/s; working electrode, vapor deposited Au (0.34 cm^2); solvent, DMF (0.1 M TBAP); concentration of reactants, 25 mM YI_3 + 75 mM N_2O. Solid line represents the background in 21 mM YI_3.

troreduction of common O-atom donors, generating species that serve as "oxide donors". In the presence of Y(III) precursors this results in deposition of Y_2O_3. Specifically, nitrous oxide (N_2O) is used as a reducible oxide donor. An attractive feature of N_2O for this purpose is the noninterfering byproduct (N_2) generated after oxide delivery.

Figure 1a shows the cyclic voltammogram (CV) for N_2O for a potential scan between 0 V and −3.5 V versus Pt (QRE). A cathodic wave is observed at −3.1 V corresponding to reduction of N_2O.[19] During the positive, return scan no reoxidation of the reduced product is observed, showing that the N_2O reduction is chemically irreversible under these conditions. Instead, two smaller anodic peaks are observed at −1.07 V and −0.62 V. These increase with N_2O concentration, indicating that they result from N_2O reduction. The larger anodic peak at −0.62 V is attributed to oxidation of superoxide, which is the major reaction product of N_2O reduction under these conditions.[19] Figure 1b shows CVs for a solution containing only YI_3 (background, solid line) and for one containing both N_2O and YI_3 (dotted line). The background shows a very small irreversible prewave at −1.02 V when the potential is scanned in the negative direction. This prewave is attributed to reduction of chemisorbed iodide adatoms (I_{ads}) to the iodide anion (I^-) on the Au substrate.[20] Low background currents are observed over the remainder of the scan range. In presence of both N_2O and YI_3 a larger peak is observed at this same potential. This peak has the symmetric shape of a surface wave and is also attributed to iodine desorption. A larger reduction process is observed beginning at −1.7 V, with the current increasing monotonically as the potential is made more negative. A broad reduction feature is observed between approximately −1.75 V and −2.5 V. These potentials are approximately 1 V positive of the N_2O reduction peak in the absence of YI_3. Repeated scanning over this potential range results in decreasing reduction current and deposition of visible films on the electrode surface. Notably, there is no distinct peak at −3.1 V, where one was observed for N_2O reduction in Figure 1a. This suggests that a new species is formed in solutions containing both N_2O and YI_3 and that this species is reducible in this range of potential.

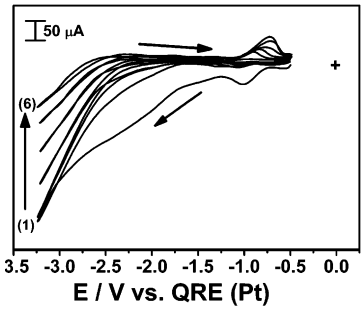

Figure 2. Successive CVs from −0.5 to −3.25 V. Scan rate, 200 mV/s; working electrode, vapor deposited Au electrode (0.34 cm^2); solvent, DMF (0.1 M TBAP); concentration of reactants, 25 mM YI_3 + 75 mM N_2O; temperature, 10−12 °C.

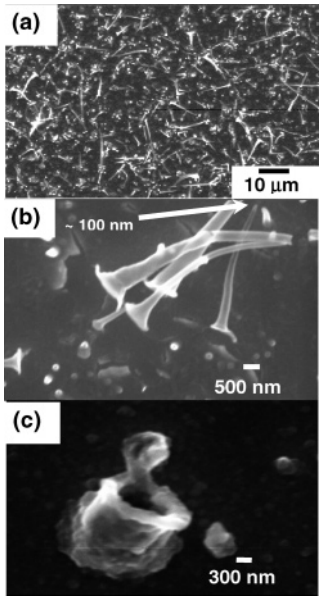

Figure 3. SEM images of (a) deposit by the cyclic voltammetric method (uniform, horn-shaped nanotubes), (b) horn-shaped nanotubes observed at higher magnification, and (c) cylindrical hollow nanostructure which eventually forms horn shaped structures. These images were obtained for the sample synthesized in DMF (0.1 M TBAP) in the presence 25 mM YI_3 and 75 mM N_2O at a scan rate of 200 mV/s at 10−12 °C.

Figure 2 shows current−potential curves for six successive scans in a solution containing 25 mM YI_3 and 75 mM N_2O. The electrochemical cell was held at lower temperatures (10−12 °C) for these cyclic voltammetric deposition experiments (see Supporting Information). The decrease in current during repeated scanning shows that deposition of an insulating material occurs. Deposition is confirmed by scanning electron micrographs (SEMs) of the surface, as shown in Figure 3. During the positive going scan one also observes the growth of an anodic peak at approximately −0.7 V, attributed to oxidation of either superoxide or iodide, both of which are reduction products.

SEMs of the deposits show the formation of uniform, horn-shaped nanotubes ("nanohorns") with a narrow size distribution coexisting with small nodular deposits (Figure 3a). Higher magnification (Figure 3b) shows the structures of the horn-shaped structures, especially the fact that they are hollow. The diameter of these structures tapers from ap-

(19) Floate, S.; Hahn, C. E. W. *J. Electroanal. Chem.* **2005**, *583*, 203−211.
(20) Soriaga, M. P. *Chem. Rev.* **1990**, *90*, 771−793.

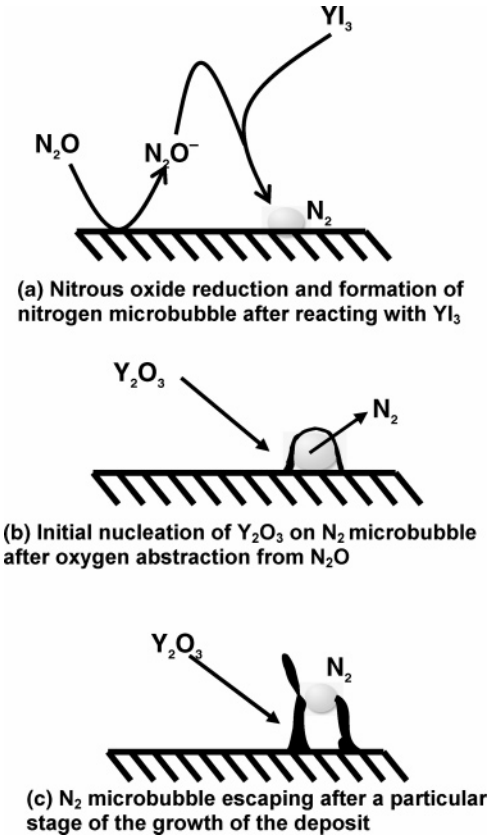

Figure 4. Schematic depiction for a possible mechanism for the formation of hollow nanocyclindrical structures.

proximately 900 nm at the base to less than 100 nm at the tip. The smallest structure in Figure 3b has a base diameter of 450 nm and a tip diameter of 80 nm. Inspection of many such images reveals that the larger base is the point of attachment to the electrode surface at the end of the deposition. The "nanohorns" had lengths ranging from 3.9 to 16.5 μm. Figure 3c shows a hollow nanocylindrical structure of the base diameter of approximately 900 nm. The thickness of the walls of the cylinder is approximately 250 nm, and the inner diameter is approximately 400 nm. These "open cap" structures have diameters similar to the nanohorn base diameters and are commonly observed at the initial stages of growth. This suggests that these open cap structures eventually grow into the nanohorns.

Figure 4 shows a speculative mechanism for the formation of the open cap structures. The reduction of N_2O produces N_2, which is present well above its saturation concentration.[21−23] This may produce a microbubble of N_2 that is adsorbed (nucleated) at the electrode surface. We note in this regard that these nanotubes are produced only on vapor deposited gold electrodes, which have chromium as the underlying adhesive layer on glass substrates. Many attempts to produce similar structures on pure Au disk electrodes were unsuccessful. Thus, we believe that specific features of the vapor deposited Au electrodes influence the structure of the deposits. Such features may include the size of Au polycrystallites and the possible presence of Cr (or Cr oxides or hydroxides) around the periphery of the polycrystallites. If the reduction processes that produce the microbubble are localized at specific nucleation sites on the surface, it seems likely that Y_2O_3 deposition might occur near the microbubble. Thus, in Figure 4b, we speculate that nucleation and growth of this deposit occur around the periphery of the microbubble. Finally, the open cap structure seen in Figure 3c is thought to be produced during escape of the microbubble after the deposition has proceeded to a critical stage, as shown in Figure 4c. In some cases, these objects appear to nucleate nanotubes, although the manner in which this occurs is not clear. However, formation of hollow cylinders and/or nanotubes requires that deposition occur only at the periphery of the base, not inside. This proposed mechanism is similar to that suggested by Qu and co-workers for producing similarly shaped, though somewhat larger, polypyrrole microcontainers.[24−26]

Other electrodeposition conditions also have been investigated as described in the Supporting Information. Nanohorns were only produced with cyclic voltammetric (scanning) conditions. Lower concentrations of either YI_3 or N_2O produced less deposition, with more microcontainers and less nanohorns. For example, with YI_3 and N_2O at 10 mM and 30 mM, respectively, the nanohorns were smaller and less abundant. Under some conditions thin, continuous films of Y_2O_3 can be deposited using this technique. The potential utility of such an approach for electrodeposition of thin dielectric films is currently being explored.

Acknowledgment. This work was supported by National Science Foundation Grant EPS-0083030.

Supporting Information Available: Experimental procedures and wavelength dispersive spectroscopy on the elemental abundance in the nanotubes (PDF). This material is available free of charge via the Internet at http://pubs.acs.org.

CM061024T

(21) Attard, G. A.; Ahmadi, A. *J. Electroanal. Chem.* **1995**, *389*, 175−190.
(22) Ahmadi, A.; Bracey, E.; Evans, R. W.; Attard, G. *J. Electroanal. Chem.* **1993**, *350*, 297−316.
(23) Bayachou, M.; Elkbir, L.; Farmer, P. J. *Inorg. Chem.* **2000**, *39*, 289−293.
(24) Qu, L.; Shi, G.; Chen, F. E.; Zhang, J. *Macromolecules* **2003**, *36*, 1063−1067.
(25) Qu, L.; Shi, G.; Yuan, J.; Han, G.; Chen, F. E. *J. Electroanal. Chem.* **2004**, *561*, 149−156.
(26) Yuan, J.; Qu, L.; Zhang, D.; Shi, G. *Chem. Commun. (Cambridge, U.K.)* **2004**, 994−995.